AD-A194 229

DOCUMENTATION PAGE

Form Approved
OMB No. 0704-0188

1a REPORT SECURITY CLASSIFICATION Unclassified		1b RESTRICTIVE MARKINGS	
2a SECURITY CLASSIFICATION AUTHORITY		3 DISTRIBUTION / AVAILABILITY OF REPORT	
2b DECLASSIFICATION DOWNGRADING SCHEDULE		Approved for public release: distribution unlimited	
4 PERFORMING ORGANIZATION REPORT NUMBER(S)		5 MONITORING ORGANIZATION REPORT NUMBER(S)	
6a NAME OF PERFORMING ORGANIZATION University of California	6b OFFICE SYMBOL (If applicable)	7a NAME OF MONITORING ORGANIZATION Office of Naval Research	
6c ADDRESS (City, State and ZIP Code) 6532-Boelter Hall, Dept of Matls Science and Engr. Los Angeles, CA 90024-1595		7b ADDRESS (City, State, and ZIP Code) Physics Division Code 1112 Arlington, VA 22217-5000	
8a NAME OF FUNDING SPONSORING ORGANIZATION	8b OFFICE SYMBOL (If applicable)	9 PROCUREMENT INSTRUMENT IDENTIFICATION NUMBER N00014-81-K0011	

8c ADDRESS (City, State and ZIP Code)	10 SOURCE OF FUNDING NUMBERS			
	PROGRAM ELEMENT NO 61153N11	PROJECT NO	TASK NO 4126700	WORK UNIT ACCESSION NO

11 TITLE (Include Security Classification)

Detection of Irradiation Effects on Reactor Vessel Steels by Magneto-Acoustic Emission

12 PERSONAL AUTHOR(S)
O-Y Kwon, K. Ono, G.E. Lucas, and G.R. Odette

13a TYPE OF REPORT Technical	13b TIME COVERED FROM 1987 TO 1988	14 DATE OF REPORT (Year, Month, Day) 19880421	15 PAGE COUNT 8

16 SUPPLEMENTARY NOTATION

17	COSATI CODES		18 SUBJECT TERMS (Continue on reverse if necessary and identify by block number)
FIELD	GROUP	SUB-GROUP	

19 ABSTRACT (Continue on reverse if necessary and identify by block number)

See the next page

DTIC
ELECTE
APR 2 6 1988
S D
H

Unclassified

Detection of Irradiation Effects on Reactor Vessel Steels by Magneto-Acoustic Emission

Oh-Yang Kwon and Kanji Ono
Department of Materials Science and Engineering, University of California, Los Angeles, Calif.
and
Glenn E. Lucas and G. Robert Oddette
Department of Chemical and Nuclear Engineering, University of California, Santa Barbara, Calif.

Abstract

The irradiation effects of reactor vessel steels were studied by magneto-acoustic emission (MAE). MAE is a new method of non-destructive evaluation. It is generated primarily by domain wall motions during magnetization of ferromagnetic materials in the alternating magnetic field. Since MAE activity is sensitive to the microstructural changes, it is applied to determine the status of steel samples exposed to neutron irradiation.

Two commercial steels, A302B plate and A533B weld, and two model alloys were irradiated at four different conditions; high and low flux, two fluence levels (0.5 or 1 x 10^{19} n/cm^2) and three temperatures (271; 288 and 307°C). For each material/condition and unirradiated control samples, MAE intensity in rms voltage with increasing magnetic field was measured. Direct and envelope-detected MAE waveforms were also recorded. Measurements were also made for the samples unirradiated but aged at 288°C up to 278 hours in order to separate the effects of thermal aging from irradiation effects. Barkhausen effects were also investigated using a surface probe. All the magnetization was at 60 Hz and waveform data was obtained at 32 kA/m rms magnetic field intensity.

The MAE intensity measurements showed effects of irradiation, but Barkhausen intensity did not. MAE waveforms changed systematically in most of the conditions. Barkhausen waveforms exhibited much smaller changes, especially in low nickel compositions. Both MAE and Barkhausen waveforms showed double peaks during each half-cycle of magnetization. While the Barkhausen waveforms could not indicate irradiation effects, MAE waveforms exhibited substantial variations. Both peak height and peak positions were affected by neutron irradiation.

The results presented here show that MAE waveform analysis can be a promising non-destructive evaluation technique for monitoring the microscopic changes in the steel components subjected to neutron irradiation.

THE RADIATION DAMAGE of a reactor vessel steel by high-energy nuclear radiation originates from the modification of its microstructure at the atomic level. The affected microstructure degrades the mechanical properties, some of which are critical to the structural integrity of reactor vessels. The primary concern of great significance is the catastrophic failure by brittle crack propagation.

Various test procedures have been developed to evaluate the embrittlement behavior of steels under controlled irradiations. Mechanical testing methods are centered on measurement of the ductile-to-brittle transition temperature. Other methods such as fracture toughness K_{Ic}, microhardness and tensile test have also been used [1]. In addition, transmission electron microscopy has been also extensively used to study the basic mechanism of irradiation embrittlement. Although these methods can provide valuable information on radiation damage and an effective means to prevent catastrophic failures by controlling microstructures, they are destructive testing and cannot be applied to the reactor in operation.

A number of nondestructive testing methods have been developed for the structure integrity of reactor components primarily to determine the presence and size of cracks. These include: ultrasonic, radiographic, eddy current, and acoustic emission testing [2]. While the detection of cracks is important for assuring the reliability and safety of nuclear reactors, it is also important to determine the microstructural changes causing embrittlement. No such method has been found.

Since magneto-acoustic emission (MAE) activity is sensitive to the microstructural changes [3-9], it is applied to determine the status of steel samples exposed to neutron irradiation. Recently, MAE was employed to examine the mechanisms of neutron irradiation damage of alpha-iron [10]. It showed that MAE responses can be correlated with the metallurgical conditions of alpha-iron. MAE can provide the bulk properties of materials since the penetration depth is at least an order-of-magnitude greater than other methods at 60 Hz magnetization [5]. This can be a special benefit in appli- cation environments where the condition of near surface layer is often quite different from the bulk.

The present study has attempted to correlate the MAE responses of reactor vessel steels with the microstructural changes due to neutron irradiation. Surface Barkhausen noise (SBN) signals were also measured to supplement this study, although little additional information has been uncovered.

EXPERIMENT AND DATA PROCESSING

MATERIALS - Samples of two commercial steels, A302B

Table 1 Chemical compositions of irradiated alloys
(percent by weight)

C	Cu	Ni	Mn	Si	P	S	Cr	Mo	V	Fe
Alloy A - A302B steel plate										
0.23	0.20	0.17	1.47	0.26	0.013	0.024	0.050	0.52	0.004	Bal.
Alloy D - A533B steel weld (EPRI Linde 0091)										
0.12	0.40	0.60	1.36	0.51	0.006	0.013	0.044	0.44	.....	Bal.
Alloy L - A model alloy										
0.10	0.28	<0.01	<0.01	<0.01	<0.02	<0.01	<0.01	....	<0.01	Bal.
Alloy S - A model alloy										
0.10	0.35	0.54	<0.008	<0.07	<0.007	<0.004	<0.003	....	<0.006	Bal.

Table 2 Designations for irradiation and aging conditions

Alloy	Designation	Description	Neutron Flux $(n/cm^2 \cdot s)$	Neutron Fluence (n/cm^2)	Temperature $(^\circ C)$	Time (hr)
A, D	00	As-received	---	---	*	*
L, S	00	Solutionized	---	---	‡	‡
All	10	Aged	---	---	288	278
All	11	Aged	---	---	288	555
All	22	Irradiated	5×10^{12}	0.5×10^{19}	288	278
All	23	Irradiated	5×10^{12}	0.5×10^{19}	307	278
All	33	Irradiated	0.5×10^{12}	0.5×10^{19}	307	2778
All	34	Irradiated	0.5×10^{12}	1×10^{19}	270	5555

* As-received conditions
Plate A: Normalized at 913±42°C; Austenitized at 871±42°C for 4 hours
Quenched in water; Tempered at 663±14°C for 4 hours; Cooled in the furnace
Stress-relieved at 607±14°C for 40 hours
Weld D: The above plus post-weld heat treatment (PWHT) at 621±14°C for 50 hours
‡ Solution treatment at 750°C, 1 hr; Forced-air quenched.

plate (designated as A) and A533B weld (as D), and of two model alloys (as L and S) were obtained in the variously irradiated conditions. Chemical compositions of materials are given in Table 1 whereas the irradiation or thermal aging conditions are summarized in Table 2. Model alloys are almost pure ternary alloy L (Fe-C-Cu) and quarternary alloy S (Fe-C-Cu-Ni), whereas the commercial steels contain various impurities and some alloying elements like Mn in both steel A and weld D. A major difference between A and D, or L and S is the copper and nickel contents.

Samples were obtained from the Department of Chemical and Nuclear Engineering, University of California, Santa Barbara. Those were irradiated in the University of Virginia Research Reactor (UVAR). Designations and some complementary informations can be found in the related literature [11-14]. All the samples were the coupons whose dimension were 38 mm long, 22 mm wide and 0.5 mm thick. As-received condition of A302B plate (A00) was normalized at 913±42°C then austenitized at 871±42°C for hours followed by water quenching, then tempered at 663 ±14°C for 4 hours followed by furnace cooling, and stress-relieved at 607±14°C for 40 hours. A533B weld (D00) had the same history as A00 except the additional post-weld heat treatment at 621±14°C for 25 hours. The model alloys were cast from double vacuum melted stock then hot rolled. As-received conditions were annealed at 857°C for 0.5 hour after final cold rolling into 0.5 mm thick sheets. Therefore, the representative microstructures were bainitic for the commercial steels and recrystallized for the model alloys.

Model alloys were given an additional heat treatment at 750°C for 1 hour followed by forced-air quench (L00 and

S00) before being subjected to the irradiation or thermal aging. This was done to ensure that copper was initially solution [11]. An initial distribution of fine carbides beli to be epsilon carbides resulted in the matrix [14]. Sampl were aged at 288°C for 10^6 sec or 278 hours (referred a and of 2×10^6 sec or 555 hours (as 11) to separate the effects of thermal aging from irradiation effects. All the h treatments were performed under vacuum and samples w prepared with No.1 microfinish after each additional hea treatment.

MAE Data Acquisition and Processing - MAE measure-ment utilized a U-core electromagnet energized by 60 Hz alternating current through a variac. Magnetic field inten was monitored by a gaussmeter (RFL Industries; Model 750) with Hall probes. A specimen was placed on top o electromagnet which is covered by a layer of elastomeric vibration insulator. An AE transducer was placed on the surface of the sample, while an SBN sensor was attache the bottom surface which faced the electromagnet. The A transducer was acoustically coupled with viscous resin whereas there was a minimal air gap between the sample surface and SBN sensor. A quasi-wideband AE sensor w employed (Model MAC-425L; AET Corp., Sacramento, CA). It was connected to a preamplifier (AET 160) that included a bandpass filter (125-1000 kHz). The SBN sensor was a flat coil of 20 turns, 7 mm in diameter mad 0.1 mm thick magnet wire, which was mounted on a 1 m thick PMMA plate. The SBN signal was also fed to the same preamplifier except with a bandpass filter of 125- 2 kHz.

For each alloy of as-received, thermally aged and th

Oh-Yang Kwon and others

irradiated condition, intensities in rms voltage were measured with increasing magnetic field. The intensities of MAE and SBN signals were monitored at preamplifier output stage using an rms voltmeter (HP 3400A). Real-time plots of intensity versus magnetic field were made by using an X-Y recorder. For waveform analysis, signal was further amplified by a main amplifier (AET 201) then fed to a full-wave integrating rectifier to obtain an envelope. All the waveforms were recorded at 32 kA/m rms magnetic field intensity. Envelopes were averaged 1024 times by using a transient recorder with signal averaging capability (Data 6000A, Analogic Corp., Danvers, MA). The sampling interval was 20 μs and 512 data points were used for an envelope which can cover a magnetic half-cycle of 8.3 ms duration. Five envelopes were recorded for each combination of specimen, magnetic field, and transducer. The obtained data were transmitted to a microcomputer (CP/M S-100 with 10 MB Iomega drive, later replaced by IBM-PC/AT) where they were stored on a hard disk and processed subsequently. Most of the waveforms were also plotted on a graphics plotter (HP 7470A) directly from the transient recorder.

In order to eliminate the effect of coupling and intensity variation, each envelope was normalized by the peak amplitude. Thus, only the shape of envelope was employed as a pattern in classifying waveforms. To form a feature set vector of 32 elements, segment averages of 16 consecutive data points out of 512 points were calculated.

For the pattern recognition analysis a reference must be prepared for each class of physically different states or processes. The dimension of the reference vectors should be identical to the number of elements in the pattern vector of measured data. The classification of waveforms was performed under the k-th nearest neighbor decision rule (kNNDR). Euclidean distances in the 32 dimensional space were calculated between a pattern vector and the references. A few programs were written in either FORTRAN or BASIC for this and other preliminary data processing. Typically, five nearest neighbors were printed out at the end of calculation. The number of the first nearest neighbor classified into each reference vector is then printed in a confusion matrix form. When identification is perfect, one can expect a diagonal matrix.

RESULTS AND DISCUSSION

MAE and BN Activities - Thermal aging at 288°C did not produce any noticeable change in MAE intensity of unirradiated steel A whose microstructure had already been stabilized by a series of heat treatments. This is shown in Figure 1 where almost a single curve was formed from the intensity measurements of A00, A10 and A11 conditions. Note that the aging condition A10 was chosen to be at the same time and temperature as the irradiated condition A22, shown in Figure 2. Any difference between A10 and A22 is thus generated by the effects of irradiation. Figure 2 shows that these are almost identical at lower magnetic fields, but the irradiation causes a slight decrease in MAE intensity at higher magnetic field. The reduction of MAE intensity was essentially the same for A22 and A23, the latter with a higher irradiation temperature of 307°C. In the condition A33 which was irradiated at a lower dose rate and a higher temperature (307°C) for 2778 hours, a significant (20% at 80 kA/m) reduction was observed. In contrast, the MAE intensity of A34 reached a level slightly higher than that of A10. This sample was irradiated to twice the fluence (to 10^{19} n/cm²) at the lowest temperature (270°C) for a longer
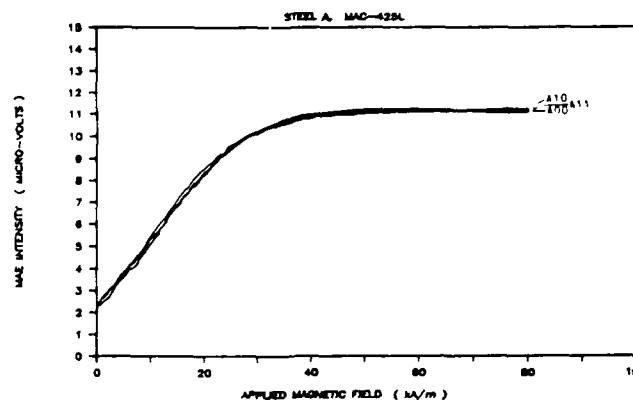

Fig. 1   Effect of thermal aging at 288°C on MAE intensity of steel A.
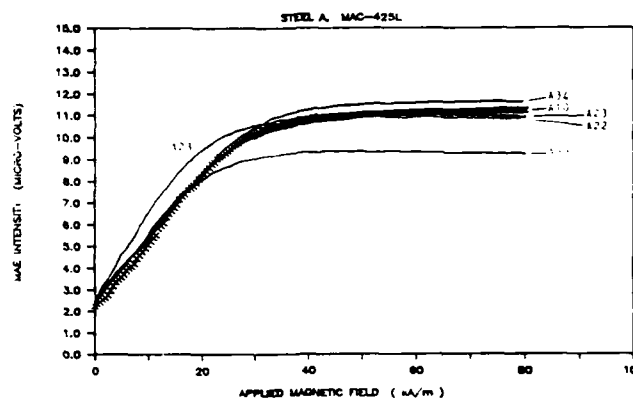

Fig. 2   Effect of neutron irradiation conditions on MAE intensity of Steel A.

duration (5555 hours).

Similar observation was made for weld D. MAE intensity of unirradiated steel D increased by the aging at 288°C for 278 hours as much as 10 percent but no further increment resulted from prolonged aging up to 555 hours. MAE intensities from the irradiated steel D varied almost the same way as those of steel A except there was a quite significant increase for the condition D23. The smaller (in steel A) and the larger (in steel D) increment in MAE intensity between conditions D22 and D23 may be attributed to the composition dependence of the sensitivity to neutron irradiation, as the welds are expected to exhibit a higher variability in alloy composition. The overall increase of MAE intensity from condition 22's and 23's can be the effects of irradiation temperature. The less homogeneous microstructure of weld D [11, 14] also appeared to produce larger variations in MAE intensity than in steel A. Difference was also observed in steel D between D23 and D33 which could be attributed to the effects of dose rate or flux.

MAE intensities of the model alloys (L and S) were also increased by thermal aging in the same way as that of the commercial steels. However, the various irradiation conditions produced different responses from the previously shown results for the commercial steels. A significant increase in MAE intensity resulted from irradiation in L22 over the condition L10 whereas MAE intensities for A22 were decreased from A10 as shown in Figure 2. MAE intensities were also suppressed by prolonged (5555 hours)

Oh-Yang Kwon and others

aging at a lower temperature and lower flux (L34) instead of the observed increase of intensities in the commercial steels. The response of alloy S was the same as that of alloy L except an unusual increase in intensity was found for the condition L33. Very little difference was observed between L22 and L23 or S22 and S23, implying that the effects of irradiation temperature were minimal in both alloys L and S. These results indicate that no detectable effect of irradiation temperature on MAE activity exists at about 300°C if the microstructures were homogeneous and stabilized (A, L and S). In the welded microstructure, however, a significant increase of MAE intensity resulted in D23 over that of D22.

The comparison of conditions 23 and 33 shows generally that MAE intensity decreases by the reduction in the neutron flux (except in alloy S). A part of the change may be due to thermal aging, but the microstructural variation causing MAE intensity changes is certainly dictated by the neutron flux as well as total neutron fluence.

Ignoring the effect of irradiation temperature between conditions 33 and 34 (while keeping the flux constant), the doubling of the fluence (in condition 34) always reversed the trend in MAE intensity. In alloys A, D and L, MAE intensities were the lowest in condition 33. In alloy S, the increase in MAE found in condition 33 essentially was eliminated in condition 34. These results indicate that the changes in MAE intensity is not monotonic and even the trend depends on the chemical composition (or possibly the microstructure). On the other hand, neutron irradiation does yield detectable changes in MAE intensity.

Surface BN responses of the same series of samples were determined. They were less consistent than the MAE responses. Thermal aging at 288°C for 278 hours decreased SBN intensity of steel A but increased that of steel D. Further aging at the temperature for 555 hours increased the intensity of both A and D.

The effects of irradiation are even more complicated. The intensity of SBN signals increased in steel A with the irradiation (A22) especially at lower field. The low-field activity remained high whereas the higher field activity decreased when irradiation temperature was raised (A23) and flux at this temperature were decreased (A33). Irradiation at lower temperature and prolonged time (A34) resulted almost identical curve as thermally aged (A10) condition. In steel D, irradiation suppressed SBN activity for all conditions except D33 which produced an almost identical curve as thermally aged condition (D10). There were considerable reductions in the lower-field SBN intensity of the irradiated conditions D22 and D23.

Both alloy L and alloy S showed low SBN activities and the variations were insignificant comparing to the MAE responses. There was a small increase in the low-field SBN activities of both alloys by thermal aging at 288°C for 278 hours. The various irradiation conditions appeared not to produce systematic changes in SBN activities in the model alloys. The intensities from the conditions 22, 23, 33 and 34 were either a little higher or lower than that of the condition 10.

Waveform Analysis - The envelope of both MAE and SBN waveforms produced two distinct peaks within a magnetic half-cycle of 8.3 ms. Effects of the thermal aging (A10) and the irradiation (A22) on MAE waveform are shown in Figure 3 for steel A. There was little change in the waveforms from the as-received (A00) to thermally aged (A10) conditions. This was not totally unexpected since the microstructure of steel A was stable enough not to be affected by aging at the temperature below 300°C.
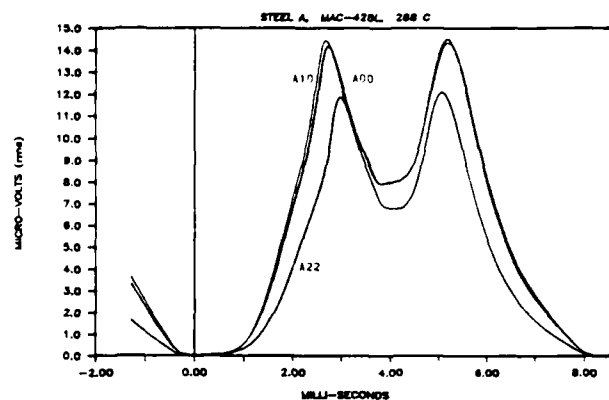

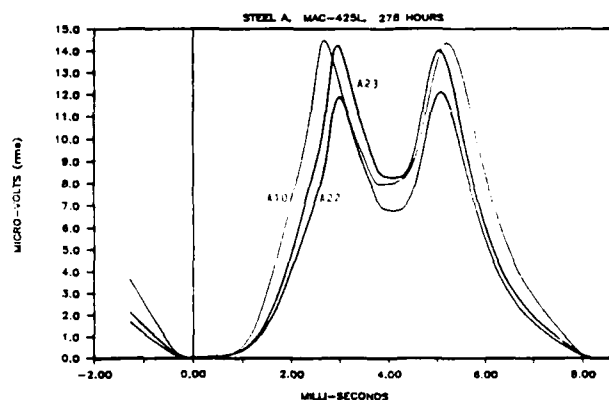Fig. 3   Effects of the thermal aging and neutron irradiati on MAE waveform of steel A.

Fig. 4   Effect of neutron irradiation temperature on MAE waveform of steel A.

On the other hand, the irradiation (A22) produced a major change in the waveform; reduction of the peak heig and shorter time interval between the peaks. Figure 4 sho the changes in waveforms between the two irradiation conditions A22 and A23. A higher irradiation temperature increased the peak heights without changing peak position or other parameters. However, a longer irradiation time (A33) suppressed MAE activities again.

Steel D produced larger variations in MAE waveform both by thermal aging and by irradiations. The microstruc ture of this weldment is still inhomogeneous in the as-received condition even though it was stress-relieved after welding. When the defective microstructure was irradiated relatively low temperature with a higher dose rate, it produced a different waveform from the others. Irradiated higher temperatures (D23 and D33) or longer periods (D3 and D34) basically recovered the consistency in waveform but in the latter case the peak heights were suppressed as the A33 or A34 conditions.

Model alloys produced an apparent dose-rate or irradiation time dependence on MAE waveforms. Figures and 6 are MAE waveform envelopes of alloy L showing t effects of irradiation and that of irradiation temperature in short-time irradiation. There was almost no change in the waveforms within the same dose rate (L22 and L23), but irradiation raised and broadened the waveforms from that thermally aged (L10). At the lower flux (L33 and 34 in Figure 6), the waveforms were suppressed, but the peak positions were the same as in other irradiated conditions.
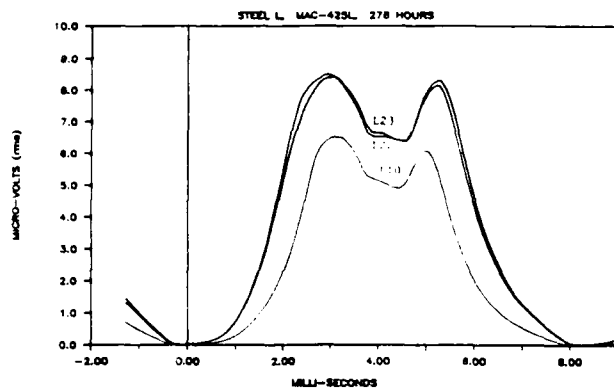
Oh-Yang Kwon and others

Fig. 5 Effect of neutron irradiation temperature on MAE waveform of steel L.
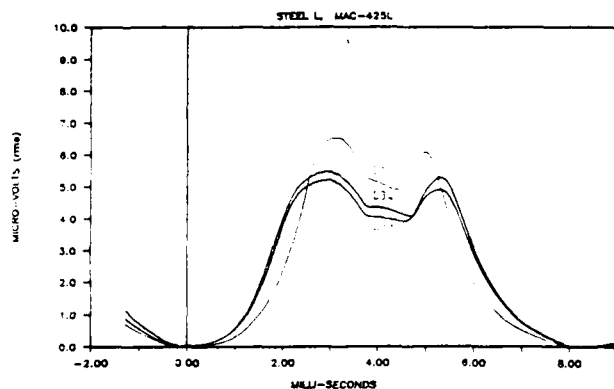

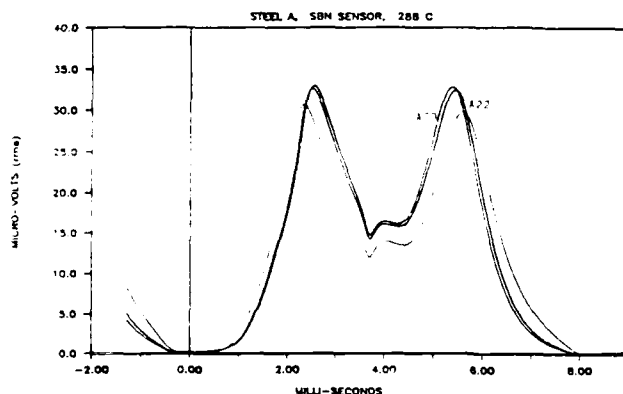Fig. 6 Effect of neutron irradiation time on MAE waveform of steel L.

Fig. 7 Effects of the thermal aging and neutron irradiation on SBN waveform of steel A.

Alloy S whose composition is higher in copper and nickel contents than alloy L also showed the same trends as the above but the difference between the classes was smaller.

SBN waveforms were affected very little by either the thermal aging or even the irradiation except in steel D. In steel A seven different conditions produced very similar waveforms. A10 waveform was lower and peak positions were wider as shown in Figure 7, but others were close to A00 and A22. On the other hand. SBN envelopes of steel D changed drastically between the conditions. Although
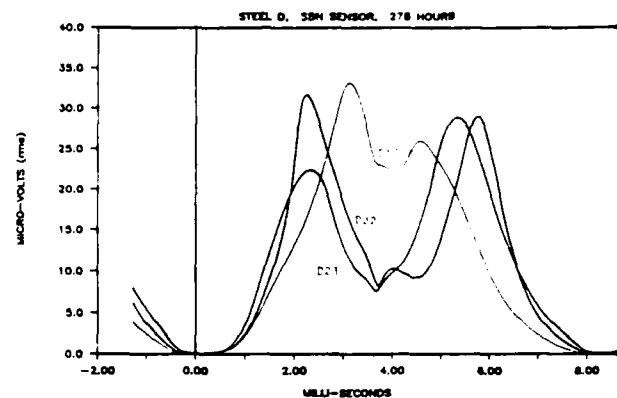

Fig. 8 Effect of neutron irradiation temperature on SBN waveform of steel D.

thermal aging did not produce much changes, the irradiati produced completely different waveforms. The condition D22 resulted in the envelope very similar to the ones of st A (Figure 8). Envelope D23 was also similar to D22 but t first peak was suppressed. With the longer aging time or dose rate, the condition D33 resulted in the waveform clo to D00 or D10. However, the first peak activity of D34 w again suppressed so that a completely different, nearly symmetric envelope was obtained. Although these results showed some clustering by dose rate or aging time, a lack consistency makes it difficult to extract trends.

The SBN waveforms from the model alloys were n much affected by various irradiation conditions. All the irradiation conditions produced similar waveforms in the alloy S as well as L. Although waveforms of thermally ag condition were different from those of irradiated conditio these results can not be utilized to determine the radiation damage in pressure vessel steels of differently irradiated conditions.

From the above results, irradiation clearly affects th MAE activities and thus the peak height of the waveforms Several parameters, for example, peak height and its posit or the skewness of the waveforms, may be utilized for the qualitative prediction of radiation damage in steels. However. most of these parameters are also affected by th applied magnetic field and the sensitivity of detecting syst including couplant between samples and sensor. Therefor the measuring system has to be under careful control. To alleviate some of the difficulties, the pattern recognition technique previously developed[15] can be utilized.

Classification by Pattern Recognition - The pattern recognition technique is applied to identify the degree of radiation damage in pressure vessel steels by utilizing the envelopes of MAE and SBN waveforms as the feature set It was found that the waveforms were kept more or less constant shape whereas the intensity or the peak height is strongly dependent on the magnetic field increment. When the feature vectors are extracted from patterns, each one is normalized to its own peak amplitude. Therefore, feature vectors has a property of invariant.

From the results discussed in the last section, there was an apparent clustering about the dose rate or irradiatio time. The references for pattern recognition were prepared by averaging two adjacent patterns which were irradiated f the same or almost same period. The individual pattern w originally recorded by real-time ensemble averaging at the transient recorder. For example, the reference A1 was th

Oh-Yang Kwon and others

5

(REFERENCES)

(TEST)	AO	A1	A2	A3	DO	D1	D2	D3	LO	L1	L2	L3	SO	S1	S2	S3
AOO	5															
A10,11		10														
A22,23			10													
A33,34				10												
DOO					5											
D10,11						9		1								
D22,23	4	1					5									
D33,34						5	2	3								
LOO									5							
L10,11										10						
L22,23											10					
L33,34												10				
SOO													5			
S10,11														3	7	
S22,23														2		8
S33,34																10

* Reference pattern designations
   0   As-received (A&D) or as-quenched (L&S)
   1   Aged at 288°C for 278 to 555 hours
   2   Irradiated at 288 or 307°C for 278 hours
   3   Irradiated for 2778 to 5555 hours
* Transducer: MAC-425L with bandpass 125-1000 kHz
* Number of elements in pattern vector: 32

Fig. 9   Determination of neutron irradiation effects by MAE waveform recognition.

mean vector between A10 and A11. Thus, the reference A1 was referred to the thermally aged, A2 to the irradiated for 10^6 sec at 288°C, and A3 to the irradiated for 10^7 sec and 2 x 10^7 sec at 307°C and 271°C, respectively. References for as-received conditions, A0, D0, L0 and S0, were actually A00, D00, L00 and S00, respectively.

The results of classification are summarized in Figure 9 for MAE waveforms. Any number at off-diagonal position indicates a misclassified data. The overall rate of 87 percent correct identifications was achieved. MAE waveforms of alloys A and L were perfectly classified with the four references, whereas those of alloy D and S lowered the overall success rate. The rate from weld D was particularly low and unacceptable. This was a little unexpected since the changes in the waveforms between conditions were larger in weld D than in plate A. This reveals that only those systematic changes are good for identifying materials status through this approach.

As discussed previously, the inhomogeneous micro structures of weld D are believed to experience complex changes when they were exposed to various condition of neutron irradiation. Although alloy S is also high in copp and nickel contents, 30 out of 35 test data were correctly identified. Model alloys were fabricated under tight contr e.g., double vacuum melting, and more or less homogeneous microstructure [14] with simpler chemical compositions.

Note that the chemistry of weld D is high in Mn, M and especially Si as well as in Cu and Ni. Silicon is one the most common elements found in nonmetallic inclusio in steels [16]. This type of nonmetallic and nonmagnetic inclusions can considerably affect the MAE responses of steel since they can be the primary obstacles to the domai wall motion. The role of this small obstacles become

Oh-Yang Kwon and others

significant for MAE activities at higher magnetization level, i.e., the Type II behavior [9].

The pattern recognition analysis for SBN waveforms resulted in the overall success rate of 78.5 percent, which was not high enough for this analysis to be utilized for identifying radiation damage in the reactor vessel steels. Comparing to MAE waveforms, the number of test data misclassified into different alloys increased as well. For example, five of the S3 (total of ten) was misclassified into L1. Thirty waveforms were misclassified out of 140 test data in total and 17 out those 30 were misclassified into different alloys. Unless this type of misclassification is overcome, the reliability of pattern recognition using SBN data is questionable. The rate of successful classification was lower for the alloys with higher copper and nickel contents (D and S) than for the alloys A and L. This reveals that an extensive study is necessary on the MAE and SBN behavior of irradiated steels with systematic changes of copper and nickel contents. The combined or interactive effects of nickel and copper on the irradiation embrittlement are not clearly understood yet. However, nickel appeared to enhance the copper related embrittlement due to 288°C radiation especially in weld metals, such as alloy D [17-19].

Due to the limited availability of samples, the composition dependence of irradiation effect on MAE or SBN responses could not be studied throughly. For example, alloys with lower copper content were also lower in nickel content and alloys with higher copper content were also higher in nickel content. Nevertheless, in the model alloys, MAE response of alloy S is quite different from that of alloy L. There is no large difference in the copper contents between the two alloys and they are much higher than 0.1% that is known as the critical value above which steels become highly sensitive to neutron irradiation [14]. Therefore, the difference in MAE behavior between alloy L and S could be attributed to the effect of nickel on the radiation hardening sensitivity.

CONCLUSIONS

1.   MAE and SBN measurements and waveform analysis through a pattern recognition technique were performed to evaluate irradiation effects on ferritic pressure vessel steels and model alloys as a fully nondestructive means.
2.   MAE intensity measurements can be utilized to detect the irradiation embrittlement of ferritic steels whereas SBN measurements showed only small changes and also hardly correlated with the irradiation conditions.
3.   Waveform analysis of MAE signals based on their envelopes can classify the degree of irradiation embrittlement of steels.
4.   Pattern recognition analysis of MAE waveforms appears to be a feasible method of nondestructive evaluation on the irradiation embrittlement of ferritic nuclear reactor vessel steels.

ACKNOWLEDGEMENT

REFERENCES

1.   L.E. Steele, Neutron Irradiation Embrittlement of Reactor Pressure Vessel Steels, Ch.6, pp. 93 - 145, International Atomic Energy Agency, Vienna, Austria, 1975.

2.   R.W. Nichols, NDE Effectiveness in Relation to R Integrity, in Quantitative NDE in the Nuclear Industry, p - 11, Proc. the Fifth International Conf. on Nondestructi Evaluation in the Nuclear Industry, R.B. Clough, ed., American Society for Metals, 1983.

3.   K. Ono and M. Shibata, Magnetomechanical AE of Iron and Steel, Mat. Eval., 38, 55 - 61, (1980).

4.   K. Ono and M. Shibata, Magnetomechanical AE fo Residual Stress and Prior Strain Determination, in Advan in Acoustic Emission, pp. 154 - 174, H.L. Dunegan and W.F. Hartman, eds., Dunhart, Knoxville, TN, 1981.

5.   K. Ono and M. Shibata and M. Man Kwan, Determination of Residual Stress by MAE, in Residual Stress Designers and Metallurgists, pp. 223 -243, L.J. Vande Walle, ed., Metals Park, OH, 1981.

6.   M. Shibata and K. Ono, MAE - New Method for Nondestructive Stress Measurement, NDT International, 227 - 234, (1981).

7.   K. Ono, Magnetomechanical Acoustic Emission - A Review, in Progress in Acoustic Emission III, pp. 200 - 212, K.Yamaguchi et al, Eds., Japan Soc. NDI, Toyko, 1986.

8.   M. Man Kwan, K. Ono and M. Shibata, Magneto-mechanical Acoustic Emission of Ferromagnetic Materials Low Magnetization Levels (Type I Behavior), J. Acousti Emission, 3, 144 - 148, (1984).

9.   M. Man Kwan, K. Ono and M. Shibata, Magneto-mechanical Acoustic Emission of Ferromagnetic Materials High Magnetization Levels (Type II Behavior), J. Acousti Emission, 3, 190 - 203, (1984).

10.   D.J. Buttle, E.A. Little, C.B. Scruby and G.A.D. Briggs, A Study of Neutron Irradiation Damage in Alpha-Iron Using Magneto-Acoustic Emission, AERE - R12332, Harwell, UK, 1987.

11.   G.E. Lucas, G.R. Odette, P.M. Lombrozo and J.W. Sheckherd, Effects of Composition, Microstructure, and Temperature on Irradiation Hardening of Pressure Vessel Steels, pp. 900-930, ASTM STP 870, American Society f Testing and Materials, Philadelphia, PA, 1985.

12.   W.L. Server and W. Oldfield, Nuclear Pressure Ves Steel Data Base, EPRI NP-933, Electric Power Research Institute, 1978.

13.   T.R. Mager, Feasibility of and Methodology for Thermal Annealing of an Embrittled Reactor Vessel, EPRI NP-2712-1, Electric Power Research Institute, 1982.

14.   G.E. Lucas, G.R. Odette, P.M. Lombrozo and J.W. Sheckherd, EPRI RP-1021/7, Electric Power Research Institute, (to be published).

15.   M. Ohtsu and K. Ono, Pattern Recognition Analysis Magnetomechanical Acoustic Emission Signals, J. Acousti Emission, 3(2), 69 - 80, (1984).

16.   R. Kiessling, The origin of nonmetallic inclusions, i Non-metallic Inclusions in Steel, Second Edition, Part III:

pp. 1 - 11. The Metals Society, London, UK, 1978.

17. J.R. Hawthorne, Significance of Nickel and Copper
Content to Radiation Sensitivity and Postirradiation Heat
Treatment Recovery of Reactor Vessel Steels, pp. 375 - 391,
ASTM STP 782, H.R. Brager and J.S. Perrin, eds.,
American Society for Testing and Materials, Philadelphia,
PA, 1982.

18. C. Guionnet et. al., Radiation Embrittlement of PWR
Reactor Vessel Weld Metals: Nickel and Copper Synergism
Effects, pp. 392 - 411, ASTM STP 782, H.R. Brager and
J.S. Perrin, eds., American Society for Testing and
Materials, Philadelphia, PA, 1982.

19. E.A. Little, Factors Controlling the Irradiation
Embrittlement Response of Low Alloy Pressure Vessel
Steels, in Dimensional Stability and Mechanical Behavior of
Irradiated Metals and Alloys, pp. 141 - 150, British Nuclear
Energy Society, London, UK, 1984.

END
DATED
FILM
8 — 88
DTIC